3092 *Inorg. Chem.* **2010**, *49*, 3092–3094
DOI: 10.1021/ic902561h

Inorganic Chemistry
Communication

$[P_3Se_7]^{3-}$: A Phosphorus-Rich Square-Ring Selenophosphate

In Chung,[†] Daniel Holmes,[‡] David P. Weliky,[‡] and Mercouri G. Kanatzidis*[,†]

[†]*Department of Chemistry, Northwestern University, Evanston, Illinois 60208, and* [‡]*Department of Chemistry, Michigan State University, East Lansing, Michigan 48824*

Received January 13, 2010

The new compound $Cs_{10}P_8Se_{20}$ features the heterotetracyclic $[P_3Se_7]^{3-}$ anion, a phosphorus-rich four-membered-ring species that possesses a P−P−P unit and formally P^{3+} and P^{4+} centers. It crystallizes in the orthorhombic space group *Pnnm* with a = 26.5456(7) Å, b = 8.0254(2) Å, c = 11.9031(4) Å, and Z = 2 at 100(2) K. The cyclic anion is cocrystallized with a $[P_2Se_6]^{4-}$ anion. Electronic absorption, Raman, Fourier transform infrared, and solid-state ^{31}P NMR spectroscopy studies of $Cs_{10}P_8Se_{20}$ are reported.

Chalcophosphates are typically ternary (A/P/Q and M/P/Q) and quaternary (A/M/P/Q) compounds with $[P_xSe_y]^{n-}$ anions in their structure, where M is a metal, A is an alkali metal, and Q is sulfur or selenium. The broad diversity of this class of compounds is attributed to various binding modes and reactivities of chalcophosphate anions in salt fluxes to coordinating metals.[1] Indeed, many selenophosphate ligands have been structurally characterized, for example, $[P_2Se_8]^{2-}$,[2] $[P_2Se_9]^{4-}$,[3] $[P_2Se_{10}]^{4-}$,[4] $[PSe_4]^{3-}\cdot 2Se_6$,[5] $[P_8Se_{18}]^{6-}$,[6] $^1_\infty[PSe_6^-]$,[7] $^1_\infty[P_2Se_6^{2-}]$,[8] α-$[P_6Se_{12}]^{4-}$,[9] β-$[P_6Se_{12}]^{4-}$, and $[P_5Se_{12}]^{5-}$.[10] The common oxidation states of phosphorus in selenophosphates are P^{4+} and P^{5+}. Because members of this family can exhibit technologically important ferroelectric,[11] nonlinear optical,[8,10,12] reversible redox chemistry relevant to secondary batteries,[13] photoluminescence,[14] and phase-change properties,[15] it is important to understand the limits of structural diversity beyond the simple $[PSe_4]^{3-}$ and $[P_2Se_6]^{4-}$ anions and how to stabilize the desirable species.

Our previous investigations of chalcophosphate compounds provided new insights into the relationship between the structure and flux composition (i.e., A:P:Se ratio).[9] We also found that excess phosphorus in the flux helps to produce less oxidized $P^{2+/3+/4+}$ species such as $A_6P_8Se_{18}$ (A = K, Rb, Cs),[6] $A_4P_6Se_{12}$ (A = Rb,[9] Cs), and $Cs_5P_5Se_{12}$.[10] In fact, except for metal phosphides,[16] compounds containing phosphorus in low formal oxidation states are largely limited to organic or organometallic species[17] such as transient phosphinidenes and their derivatives, catenated polyphosphines, and elemental P.[16]

Here we describe the novel heterocyclic anion of $[P_3Se_7]^{3-}$ found in the new compound $Cs_{10}P_8Se_{20}$.[18] The cyclic anion features a ring structure and phosphorus in two different formal oxidation states, 3+ and 4+. The ring seems highly strained with a rare P−P−P unit ($\angle$P(2)−P(1)−P(2) ∼ 90°). The $[P_3Se_7]^{3-}$ molecule cocrystallizes with the ethane-like $[P_2Se_6]^{4-}$ anion to form $Cs_{10}P_8Se_{20}$. $[P_xSe_y]^{n-}$ anions with a ring structure are uncommon, and only a few have been structurally characterized, i.e., $[P_2Se_8]^{2-}$,[2] α,β-$[P_6Se_{12}]^{4-}$,[9] and $[P_5Se_{12}]^{5-}$.[10]

*To whom correspondence should be addressed. E-mail: m-kanatzidis@northwestern.edu.

(1) Kanatzidis, M. G. *Curr. Opin. Solid State Mater. Sci.* **1997**, *2*, 139.
(2) (a) Chung, I.; Kanatzidis, M. G. $Cs_2P_2Se_8$: Unpublished results. (b) Zhao, J.; Pennington, W. T.; Kolis, J. W. *J. Chem. Soc., Chem. Commun.* **1992**, 265. (c) Rotter, C.; Schuster, M.; Kidik, M.; Schon, O.; Klapotke, T. M.; Karaghiosoff, K. *Inorg. Chem.* **2008**, *47*, 1663.
(3) Chondroudis, K.; Kanatzidis, M. G. *Inorg. Chem.* **1995**, *34*, 5401.
(4) Gave, M. A.; Canlas, C. G.; Chung, I.; Iyer, R. G.; Kanatzidis, M. G.; Weliky, D. P. *J. Solid State Chem.* **2007**, *180*, 2877.
(5) Dickerson, C. A.; Fisher, M. J.; Sykora, R. E.; Albrecht-Schmitt, T. E.; Cody, J. A. *Inorg. Chem.* **2002**, *41*, 640.
(6) Chondroudis, K.; Kanatzidis, M. G. *Inorg. Chem.* **1998**, *37*, 2582.
(7) Chung, I.; Do, J.; Canlas, C. G.; Weliky, D. P.; Kanatzidis, M. G. *Inorg. Chem.* **2004**, *43*, 2762.
(8) Chung, I.; Malliakas, C. D.; Jang, J. I.; Canlas, C. G.; Weliky, D. P.; Kanatzidis, M. G. *J. Am. Chem. Soc.* **2007**, *129*, 14996.
(9) Chung, I.; Karst, A. L.; Weliky, D. P.; Kanatzidis, M. G. *Inorg. Chem.* **2006**, *45*, 2785.
(10) Chung, I.; Jang, J. I.; Gave, M. A.; Weliky, D. P.; Kanatzidis, M. G. *Chem. Commun.* **2007**, 4998.
(11) (a) Carpentier, C. D.; Nitsche, R. *Mater. Res. Bull.* **1974**, *9*, 1097. (b) Scott, B.; Pressprich, M.; Willet, R. D.; Cleary, D. A. *J. Solid State Chem.* **1992**, *96*, 294.
(12) (a) Chung, I.; Jang, J. I.; Malliakas, C. D.; Ketterson, J. B.; Kanatzidis, M. G. *J. Am. Chem. Soc.* **2010**, *132*, 384. (b) Chung, I.; Song, J. H.; Jang, J. I.; Freeman, A. J.; Ketterson, J. B.; Kanatzidis, M. G. *J. Am. Chem. Soc.* **2009**, *131*, 2647. (c) Lacroix, P. G.; Clement, R.; Nakatani, K.; Zyss, J.; Ledoux, I. *Science* **1994**, *263*, 658.
(13) Lemehaute, A.; Ouvrard, G.; Brec, R.; Rouxel, J. *Mater. Res. Bull.* **1977**, *12*, 1191.
(14) Huang, Z. L.; Cajipe, V. B.; Lerolland, B.; Colombet, P.; Schipper, W. J.; Blasse, G. *Eur. J. Solid State Inorg. Chem.* **1992**, *29*, 1133.
(15) (a) Breshears, J. D.; Kanatzidis, M. G. *J. Am. Chem. Soc.* **2000**, *122*, 7839. (b) McCarthy, T. J.; Kanatzidis, M. G. *Chem. Mater.* **1993**, *5*, 1061. (c) McCarthy, T. J.; Kanatzidis, M. G. *Inorg. Chem.* **1995**, *34*, 1257. (d) Kanatzidis, M. G.; Huang, S. P. *Inorg. Chem.* **1989**, *28*, 4667.
(16) von Schnering, H. G.; Hönle, W. *Chem. Rev.* **1988**, *88*, 243–273.
(17) Ellis, B. D.; Macdonald, C. L. B. *Inorg. Chem.* **2006**, *45*, 6864–6874.
(18) The synthesis of $Cs_{10}P_8Se_{20}$ was achieved by reacting the 1:2:2 Cs_2Se_2/P/Se mixture under vacuum in a fused-silica tube at 600 °C for 3days followed by cooling to 250 °C at a rate of 5 °C h^{-1} and room temperature in 3 h. The products were washed with degassed *N*,*N*-dimethylformamide, acetonitrile, and ether under a N_2 atmosphere to reveal pure orange crystals of $Cs_{10}P_8Se_{20}$. The yield was ∼70% based on phosphorus. The crystals are stable in alcohol, water, and air and are slightly soluble in *N*-methylformamide.

Published on Web 02/24/2010

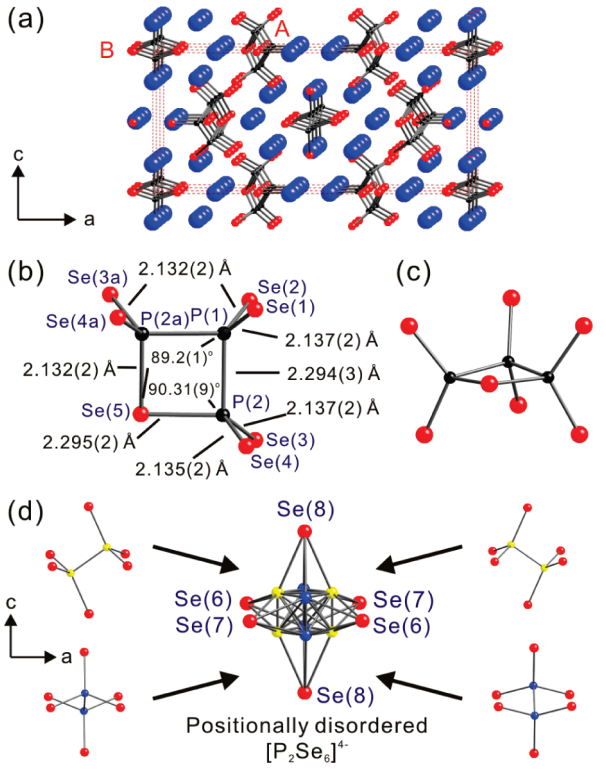

Figure 1. (a) Structure of $Cs_{10}P_8Se_{20}$ viewed down the *b* axis. The $[P_3Se_7]^{3-}$ anion is labeled as "A" and the $[P_2Se_6]^{4-}$ anion as "B". Color code: blue, Cs atoms; black, P atoms; red, Se atoms. (b and c) Structure of the $[P_3Se_7]^{3-}$ square anion. P and Se atoms are labeled. Bond distances (Å) and angles (deg) are represented. Symmetrically equivalent atoms are denoted as "a". (d) Example of an apparently complex, disordered $[P_2Se_6]^{4-}$ anion sitting on (0, 0.5, *z*), one of the special positions of the *Pnnm* space group. It is a superimposed image of four $[P_2Se_6]^{4-}$ units in different orientations that share the same center of symmetry at the special position. Color code: blue, P(3) atoms; yellow, P(4) atoms; red, Se atoms. Each Se atom is labeled.

The new structure type of $Cs_{10}P_8Se_{20}$ crystallizes in the *Pnnm* space group.[19] The compound is best described as a double salt $[Cs_3[P_3Se_7]]_2 \cdot [Cs_4[P_2Se_6]]$ and contains two discrete molecules of $[P_3Se_7]^{3-}$ (A) and one of $[P_2Se_6]^{4-}$ (B) (Figure 1a). The $[P_3Se_7]^{3-}$ anion is structurally unique, and its most unusual feature is the heterocyclic square composed of one Se atom and three P atoms. A P−P−P unit with two types of the formal charges of P^{3+} and P^{4+} are found on the ring (Figure 1b). The trivalent formal charge is found on P(1). A mirror plane bisects the noncentrosymmetric molecule to give the C_m point group, with P(2) being related with P(2a) by the reflection symmetry operation. The nearly square-planar $[P_3Se_7]^{3-}$ is slightly folded parallel to the mirror plane to form a kite shape (Figure 1b,c): ∠P(2)−P(1)−P(2), 89.2(1)°; torsion angle of P(1)−P(2)−Se(5)−P(2), 7.468°. Note that the P(2)−Se(5) distance, 2.295(2) Å, is very close to that of P(1)−P(2) at 2.294(3) Å. The P(1)−P(2) distance is significantly longer than those normally found in other chalcophosphate compounds (2.18−2.22 Å), implying the existence of strain in the four-membered ring. The stain implies a possible reactive tendency of this anion toward relieving it. For example, we expect the addition of 2 equiv of Se to $[P_3Se_7]^{3-}$ to result in the new inorganic ring species of $[P_3Se_9]^{3-}$ according to Scheme 1.

Scheme 1

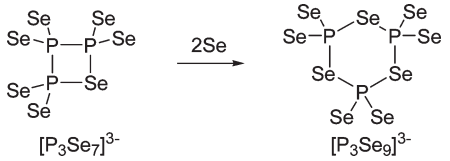

Compounds with homocyclic P_4 units have been structurally characterized, e.g., $(NH_4)_4[P_4S_8] \cdot 2H_2O$[20] and $Cs_2P_4 \cdot 2NH_3$,[21] and similarly long P−P distances were also observed in $[P_4S_8]^{4-}$ at 2.280(1) and 2.287(1) Å, which consists of four tetracoordinated P atoms with two terminal S atoms on each P atom.[20] The Se analogue to this molecule is not yet reported. Even longer P−P bond distances were found in neutral cage-like phosphorus sulfides such as P_4S_7 at 2.326(7) Å[22] and α-P_4S_4 at 2.360(3) Å.[23] Because of the four-membered ring structure of the $[P_3Se_7]^{3-}$ anion, unusually short, nonbonding intramolecular interactions are observed for P(2)···P(2a) at 3.222(3) Å, P(1)···Se(4) at 3.647(2) Å, P(1)···Se(5) at 3.254(3) Å, and Se(3)···Se(5) at 3.645(1) Å. These distances are shorter than the sum of the ionic radii of atoms.[24]

The seemingly complex, discrete anion B is a superimposed image of four positionally disordered, ethane-like $[P_2Se_6]^{4-}$ anions (Figure 1d). The site occupancy of P(3) and P(4) atoms is 25%, respectively. The $[P_2Se_6]^{4-}$ anions disorder because they reside on the fixed-symmetry elements that they do not possess, i.e., on the special positions of the *Pnnm* space group: (0, 0.5, *z*), Wyckoff position 4f, site symmetry 2; (0.5, 0, 0.5), Wyckoff position 2c, site symmetry 2/*m*. The $[P_2Se_6]^{4-}$ molecule adopts the D_{3h} point group when ideal, and the P−P bonds of the anions are tilted with respect to the crystallographic *c* axis. Because the atomic sites in the unit cell are defined by symmetry elements, the $[P_2Se_6]^{4-}$ anions that do not satisfy such site symmetries, 2 and 2/*m*, are forced to be positionally disordered. Because all Se atom positions are arranged octahedrally, they are superimposed for all orientations of the X anion. Thus, the Se atoms appear ordered, and it is only the P−P bonds that change direction. A similar symmetry-related disorder is found in $[Mo_2Cl_8]^{n-}$.[25]

The synthesis of $Cs_{10}P_8Se_{20}$ provides further insight into the close relationship between the structure and flux condition (or A:P:Se ratio) and how the low-valent P species in the alkali selenophosphate class can be stabilized. The remarkably rich structural chemistry of the Cs/P/Se system is summarized in Table 1. More basic fluxes (i.e., those with a high A:P ratio) or higher reaction temperatures tend to give shorter structural fragments[26] and phosphorus in the 5+ oxidation state. As the basicity decreases, more complex species emerge such as the one-dimensional polyselenide chains $^1_\infty[PSe_6^-]$ and $^1_\infty[P_2Se_6^{2-}]$.

(19) Crystal data for $Cs_{10}P_8Se_{20}$ at 100(2) K: STOE IPDS 2T diffractometer, Mo Kα radiation at (λ = 0.710 73 Å), orthorhombic, *Pnnm*, a = 26.5456(7) Å, b = 8.0254(2) Å, c = 11.9031(4) Å, V = 2535.8(1) Å^3, Z = 2, D_c = 4.133 g cm^{-3}, μ = 21.771 mm^{-1}, 2θ = 3.06−50.52°, 15 751 total reflections, 2242 unique reflections with R_{int} = 5.55%, GOF = 1.159, 118 parameters, R1 = 3.39%, wR2 = 7.79% for $I > 2\sigma(I)$.

(20) Falius, H.; Krause, W.; Sheldrick, W. S. *Angew. Chem., Int. Ed. Engl.* **1981**, *20*, 103.
(21) Kraus, F.; Korber, N. *Chem.—Eur. J.* **2005**, *11*, 5945.
(22) Vos, A.; Olthof, R.; Vanbolhu, F.; Botterwe, R. *Acta Crystallogr.* **1965**, *19*, 864.
(23) Griffin, A. M.; Minshall, P. C.; Sheldrick, G. M. *J. Chem. Soc., Chem. Commun.* **1976**, 809.
(24) Shannon, R. D. *Acta Crystallogr., Sect. A: Found. Crystallogr.* **1976**, *32*, 751.
(25) Cotton, F. A.; Eglin, J. L. *Inorg. Chim. Acta* **1992**, *198−200*, 13.
(26) Kanatzidis, M. G.; Sutorik, A. C. *Prog. Inorg. Chem.* **1995**, *43*, 151.

Table 1. Complex Structural Chemistry of the Cs/P/Se System: Relationship between the Observed Selenophosphate Species and the A:P:Se Ratio in the Flux[a]

compound	A:P:Se ratio[b]	anion	flux condition	color	note
Cs_3PSe_4[27]	3:1:4	$[PSe_4]^{3-}$	basic	yellow	discrete molecule
$Cs_7P_3Se_{13}$[c]	2.33:1:4.33	$[P_2Se_9]^{4-}\cdot[PSe_4]^{3-}$		red	discrete molecule
$Cs_4P_2Se_{10}$[4]	2:1:5	$[P_2Se_{10}]^{4-}$		red	discrete molecule
$Cs_4P_2Se_9$[3]	2:1:4	$[P_2Se_9]^{4-}$		red	discrete molecule
$Cs_{10}P_8Se_{20}$	1.25:1:2.5	$2[P_3Se_7]^{3-}\cdot[P_2Se_6]^{4-}$	intermediate	orange	ring included
$Cs_4P_4Se_{14}$[c]	1:1:3.5	$[P_2Se_6]^{2-}\cdot[P_2Se_8]^{2-}$		red	two-ring molecules
$Cs_4P_6Se_{12}$[10]	1:1.5:3	β-$[P_6Se_{12}]^{4-}$		orange	ring, PC[d]
$Cs_5P_5Se_{12}$[10]	1:1:2.4	$[P_5Se_{12}]^{5-}$		red	ring, PC, SHG[e]
$Cs_6P_8Se_{18}$[6]	1:1.33:3	$[P_8Se_{18}]^{6-}$		red	oligomer
"$Cs_3P_3Se_7$"[f]	1:1:2.33	$[P_3Se_7]^{3-}$			ring
$Cs_2P_2Se_8$[2a]	1:1:4	$[P_2Se_8]^{2-}$	"acidic"	orange	ring
$Cs_2P_2Se_6$	1:1:3	$^1_\infty[P_2Se_6^{2-}]$		orange	1-D, PC, SHG
$CsPSe_6$[7]	1:1:6	$^1_\infty[PSe_{6-}]$		orange	1-D, PC

[a] All compounds have been structurally refined by single-crystal diffraction. [b] These are typical ratios. In fact, there are ranges in these ratios that define a given flux condition and can lead to the compounds shown. [c] Unpublished results. [d] Crystal-glass phase-change (PC) behavior shown. [e] Nonlinear optical second-harmonic generation (SHG) response observed. [f] "$Cs_3P_3Se_7$" in $Cs_{10}P_8Se_{20}$ was represented for comparison with other cyclic selenophosphate anions.

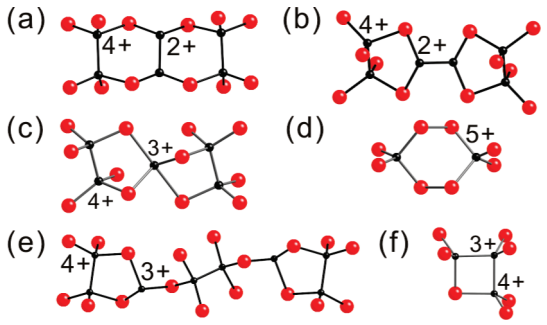

Figure 2. Examples of the selenophosphate anions isolated from intermediate/less basic flux conditions: (a) α-$[P_6Se_{12}]^{4-}$; (b) β-$[P_6Se_{12}]^{4-}$; (c) $[P_5Se_{12}]^{5-}$; (d) $[P_2Se_8]^{2-}$; (e) $[P_8Se_{18}]^{6-}$; (f) $[P_3Se_7]^{3-}$. The formal charge on P centers is represented.

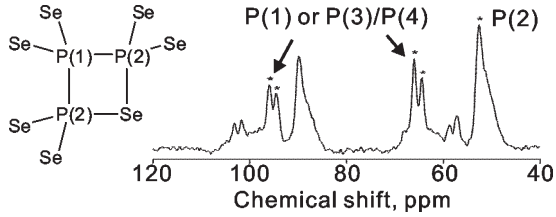

Figure 3. Solid-state ^{31}P MAS NMR spectrum of polycrystalline $Cs_{10}P_8Se_{20}$ at a 9.4 T field and a 6.0 kHz spinning frequency with the dominant isotropic peaks highlighted by asterisks. The $[P_3Se_7]^{3-}$ anion is represented.

In this work, we examined the intermediate "acidic"/basic conditions with an excess of phosphorus. If we count "$Cs_3P_3Se_7$" in $Cs_{10}P_8Se_{20}$ as an independent species, all species in those A:P:Se ranges, i.e., $[P_8Se_{18}]^{6-}$, $[P_6Se_{12}]^{4-}$, $[P_5Se_{12}]^{5-}$, and $[P_3Se_7]^{3-}$, possess the less oxidized $P^{2+/3+/4+}$ with mixed formal charge centers on P and adopt a ring-type molecular structure (Figure 2).

We could only obtain $Cs_{10}P_8Se_{20}$ by a flux reaction. Our attempts to synthesize the single salt "$Cs_3[P_3Se_7]$" by a direct combination reaction gave only $Cs_5P_5Se_{12}$,[10] which is not surprising because it is compositionally very close to $Cs_3P_3Se_7$, i.e., with the Cs:P:Se ratio being 1:1:2.33 for the former and 1:1:2.4 for the latter. A total of 1 mol of excess P (Cs_2Se_2:P:Se = 1:3:2) to the flux condition of the title compound produced a red glass.

According to differential thermal analysis performed at a rate of 10 °C min^{-1}, $Cs_{10}P_8Se_{20}$ melts incongruently at ~392 °C and the melt crystallizes at ~364 °C. The powder X-ray diffraction pattern after recrystallization indicated $Cs_{10}P_8Se_{20}$ and a small amount of orange glass. The solid-state optical absorption spectrum revealed a well-defined absorption edge at 2.07 eV, consistent with its orange color (Figure S1 in the Supporting Information). By comparison, the ring-type compounds $Cs_5P_5Se_{12}$ with $P^{3+/4+}$ and $Cs_4P_6Se_{12}$ with $P^{2+/4+}$ showed a band gap at 2.17 eV.

Solid-state ^{31}P magic angle spinning (MAS) NMR spectroscopy of polycrystalline samples of $Cs_{10}P_8Se_{20}$ gave three sets of isotropic peaks at 52.5 ppm, (64.5 +66.0) ppm, and (94.6 + 95.9) ppm (Figure 3). These peaks were identified by a comparison of spectra at different spinning frequencies, and the remaining peaks can be assigned as spinning sidebands. Considering both isotropic and spinning sideband peaks, the overall integrated intensities for the 52.5 ppm, (64.5 + 66.0) ppm, and (94.6 + 95.9) ppm peaks were ~2:1:1, which suggests an assignment of the 52.5 ppm peak to P(2), the (64.5 + 66.0) ppm peak to P(1) or P(3)/P(4), and the (94.6 + 95.9) ppm peak to the remaining P. The result supports the crystal structure of $Cs_{10}P_8Se_{20}$, which indicates three magnetically independent P atoms [P(3) and P(4) are locally and magnetically identical]. The positive isotropic shifts and overall separation of ~150 ppm between extreme splitting sidebands of peaks are consistent with P−P bonding in this compound.[28]

The molecular salt $Cs_{10}P_8Se_{20}$ stabilizes the new inorganic heterotetracyclic anion with its low-oxidation-state P^{3+} and P^{4+} centers and highly strained intraring bonds. Its discovery highlights the rich chemical diversity of the $[P_xSe_y]^{n-}$ system and the importance of the relationship between the basicity and final products.

Acknowledgment. Financial support was provided by the National Science Foundation (Grant DMR-0801855).

Supporting Information Available: X-ray crystallographic file (in CIF format), experimental details, crystallographic refinement data, and optical absorption, FT-IR, Raman, and NMR spectroscopy data. This material is available free of charge via the Internet at http://pubs.acs.org.

(27) Knaust, J. M.; Dorhout, P. K. *J. Chem. Crystallogr.* **2006**, *36*, 217.
(28) Canlas, C. G.; Kanatzidis, M. G.; Weliky, D. P. *Inorg. Chem.* **2003**, *42*, 3399.

Supporting Information

$[P_3Se_7]^{3-}$: A Phosphorus-Rich Square-selenophosphate

In Chung,[1] Daniel Holmes,[2] David P. Weliky[2] and Mercouri G. Kanatzidis[1]*

[1]*Department of Chemistry, Northwestern University, Evanston, IL 60208, USA*
[2]*Department of Chemistry, Michigan State University, East Lansing, MI 48824, USA*

* To whom correspondence should be addressed:

Prof. Mercouri G. Kanatzidis

Department of Chemistry, Northwestern University, Evanston, IL 60208

m-kanatzidis@northwestern.edu

Tel) 847-467-1541

Fax) 847-491-5937

Contents

Experimental Section

X-ray Powder Diffraction. X-ray powder diffraction analysis was performed using a calibrated CPS 120 INEL X-ray powder diffractometer (Cu Kα graphite monochromatized radiation) operating at 40 kV/20 mA and equipped with a position-sensitive detector with flat sample geometry.

Scanning Electron Microscopy. Semiquantitative analysis of the compound was obtained with a Hitachi S3400N-II scanning electron microscope (SEM) equipped with an ESED II detector.

Solid-state UV-Vis spectroscopy. Optical diffuse reflectance measurements were performed at room temperature using a Shimadzu UV-3101 PC double-beam, double-monochromator spectrophotometer operating in the 200-2500 nm region. The instrument is equipped with an integrating sphere and controlled by a personal computer. $BaSO_4$ was used as a 100% reflectance standard. The details are described elsewhere.[1]

Raman Spectroscopy. Raman spectrum was recorded on a Holoprobe Raman spectrograph equipped with a CCD camera detector using 633 nm radiation from a HeNe laser for excitation and a resolution of 4 cm^{-1}. Laser power at the sample was estimated to be about 5 mW, and the focused laser beam diameter was ca. 10 μm. A total of 128 scans was sufficient to obtain good quality spectra.

Infrared Spectroscopy. FT-IR spectrum was recorded as solids in a CsI matrix. The sample was ground with dry CsI into a fine powder and pressed into a translucent pellet. The spectra were recorded in the far-IR region (600-100 cm^{-1}, 4 cm^{-1} resolution) with the use of a Nicolet 740 FT-IR spectrometer equipped with a TGS/PE detector and silicon beam splitter.

Differential Thermal Analysis (DTA). Experiments were performed on a Shimadzu DTA-50 thermal analyzer. A sample (~30 mg) of ground crystalline material was sealed in a silica ampoule under vacuum. A similar ampoule of equal mass filled with Al_2O_3 was sealed and placed on the reference side of the detector. The sample was heated to 550°C at a rate of 10°C min^{-1}, and after 1 min it was cooled at –10 °C min^{-1} to 50 °C. The residue of the DTA experiments was examined by X-ray powder diffraction. Reproducibility of the results was confirmed by running multiple heating/cooling cycles. The melting and crystallization points were measured at onset of the endothermic peak and the exothermic peak.

MAS ^{31}P NMR spectroscopy. Bloch decay magic angle spinning ^{31}P NMR spectra of polycrystalline $Cs_{10}P_8Se_{10}$ were obtained at ambient temperature on a 9.4 T spectrometer (Varian Infinity Plus) using a 6 mm diameter rotor, spinning frequency of 5.0 or 6.0 kHz, ^{31}P frequency of 161.8 MHz, 15 μs $\pi/2$ pulse, and 1000 s recycle delay. Each spectrum was the sum of four scans and was referenced to phosphoric acid at 0 ppm. Each spectrum was processed with 50 Hz Gaussian line broadening and baseline correction.

X-ray Crystallography. Intensity data for $Cs_{10}P_8Se_{20}$ were collected at 100(2) K on a STOE IPDS 2T diffractometer with Mo Kα radiation operating at 50 kV and 30 mA with a 34 cm diameter imaging plate. Individual frames were collected with a 11 min exposure time and a 1.0 ω rotation. The X-AREA, X-RED and X-SHAPE software package was used for data extraction and integration and to apply empirical and analytical absorption corrections (crystal dimension: 0.167 × 0.118 × 0.014 mm^3). The SHELXTL software package was used to solve and refine the structure. The most satisfactory refinement was obtained with the centrosymmetric space group, *Pnnm*. All atoms were refined anisotropically. The Cs(4) atom was modeled as split into Cs(4A) and Cs(4B) sites. Their occupancy ratio was refined to 7:3. The site occupancy of the P(3) and P(4) atoms was refined to 25 %, respectively. All other atoms were refined to full occupancy. The parameters for data collection and the details of the structural refinement are given in Table S1. Fractional atomic coordinates and displacement parameters are given in Tables S2 and S3.

Table S1. Crystallographic Refinement Details for $Cs_{10}P_8Se_{20}$.

Formula	$Cs_{10}P_8Se_{20}$
Crystal system	Orthorhombic
Space group	*Pnnm* (no. 58)
Unit cell dimensions,	a = 26.5456(7) Å
	b = 8.0254(2) Å
	c = 11.9031(4) Å
Z	2
V, Å^3	2535.8(1)
d (calculated), gr cm^{-3}	4.133
Crystal dimensions, mm^3	0.167 × 0.118 × 0.014
Temperature, K	100(2)
λ, Å	0.71073
μ, mm^{-1}	21.711
F(000)	2700
θ_{max}, deg	25.26
Total/unique reflections	15751/2242
R_{int}	0.0555
No. Parameters	118
Refinement method	Full-matrix least-squares on F^2
Final R indices [$I > 2\sigma(I)$], R_1[a]/wR_2[b]	0.0339 / 0.0779
R indices (all data), R_1/wR_2	0.0391 / 0.0800
Goodness-of-fit on F^2	1.159
Largest diff. peak and hole	0.793/-1.789 eA^{3-}

[a] $R_1 = \sum ||F_o| - |F_c|| / \sum |F_o|$. [b] $wR_2 = \{\sum [w(F_o^2 - F_c^2)^2] / \sum [w(F_o^2)^2]\}^{1/2}$

Table S2. Atomic coordinates ($\times 10^4$) and equivalent isotropic displacement parameters ($Å^2 \times 10^3$) for $Cs_{10}P_8Se_{20}$ at 100(2) K. U_{eq} is defined as one third of the trace of the orthogonalized U_{ij} tensor.

	x	*y*	*z*	U_{eq}
Cs(1)	1986(1)	497(1)	0	29(1)
Cs(2)	611(1)	3197(1)	5000	32(1)
Cs(3)	0	0	2057(1)	44(1)
Cs(4A)	1349(2)	5567(3)	1991(1)	27(1)
Cs(4B)	1482(2)	5585(8)	2124(5)	27(1)
Se(1)	3316(1)	750(1)	0	30(1)
Se(2)	4365(1)	3668(2)	0	29(1)
Se(3)	3697(1)	6095(1)	2416(1)	31(1)
Se(4)	2592(1)	3416(1)	2416(1)	29(1)
Se(5)	2867(1)	6596(1)	0	31(1)
Se(6)	762(1)	2768(2)	0	29(1)
Se(7)	653(1)	7610(2)	0	38(1)
Se(8)	0	5000	2293(1)	45(1)
P(1)	4918(4)	2500	2978(3)	10(1)
P(2)	4927(1)	2500	7169(3)	11(1)
P(3)	7054(1)	2500	1014(1)	13(1)
P(4)	8481(1)	2500	7335(1)	15(1)

The occupancies of Cs(4A), Cs(4B), P(3) and P(4) are 70%, 30%, 25% and 25%, respectively. All other atoms are fully occupied.

Table S3. Selected Bond Distances (Å) and Angles (°) for $Cs_{10}P_8Se_{20}$ at 100(2) K.

P(1)-P(2)	2.294(3)	P(1)···P(4)	3.647(2)
P(3)-P(3)	2.264(16)	P(1)···P(5)	3.254(3)
P(4)-P(4)	2.237(16)	P(2)···P(2)	3.222(3)
P(1)-Se(1)	2.137(3)	P(3)···P(5)	3.645(1)
P(1)-Se(2)	2.132(3)		
P(2)-Se(3)	2.137(2)	P(2)-P(1)-P(2)	89.2(1)
P(2)-Se(4)	2.135(2)	P(1)-P(2)-Se(5)	90.31(9)
P(2)-Se(5)	2.295(2)	P(2)-Se(5)-P(2)	89.2(1)
P(3)-Se(6)	2.220(7)	Se(1)-P(1)-Se(2)	116.9(1)
P(3)-Se(7)	2.241(8)	Se(3)-P(2)-Se(4)	117.5(1)
P(3)-Se(8)	2.292(7)	Se(1)-P(1)-P(2)	111.7(1)
P(4)-Se(6)	2.257(8)	Se(2)-P(1)-P(2)	112.1(1)
P(4)-Se(7)	2.290(8)		
P(4)-Se(8)	2.267(8)		

Figure S1. Solid-state electronic optical absorption spectrum of $Cs_{10}P_8Se_{20}$.

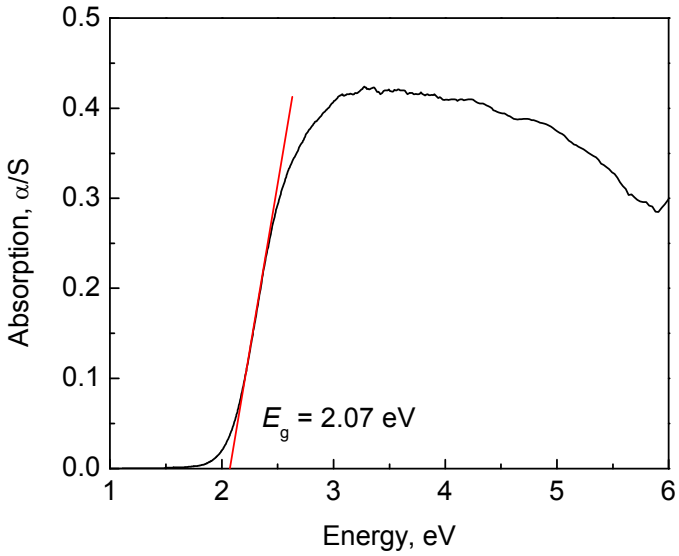

Figure S2. The Raman spectrum of $Cs_{10}P_8Se_{20}$ shows shifts at 184(w), 214(vs), 254(w), 299(vw), 340(w), 351(w), 370(w), 457(w), 492(w), and 502(w) cm^{-1}. Peak positions are similar to those of selenophosphate cyclic molecules with low valent P such as $Rb_4P_6Se_{12}$,[2] $Cs_5P_5Se_{12}$, and $Cs_4P_6Se_{12}$.[3]

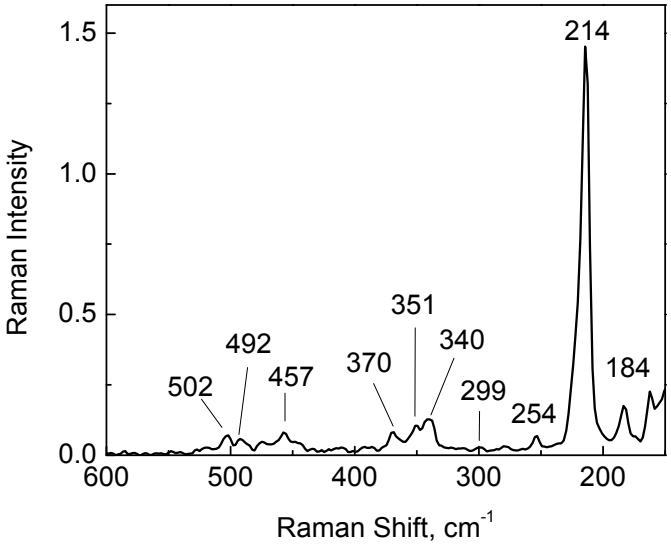

Figure S3. FT far-IR spectrum of $Cs_{10}P_8Se_{20}$.

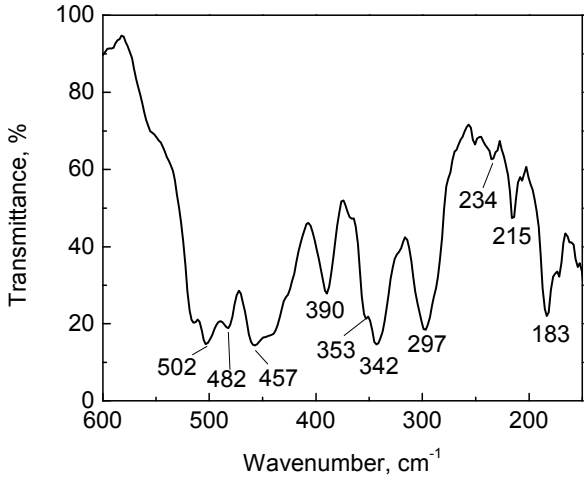

Figure S4. MAS ^{31}P solid-state NMR spectrum of polycrystalline $Cs_{10}P_8Se_{20}$ at 9.4 T field and 6.0 kHz spinning frequency. Panel (a) displays the full spectrum and panel (b) is an inset with the dominant isotropic peaks highlighted by asterisks. The $[P_3Se_7]^{3-}$ anion is represented.

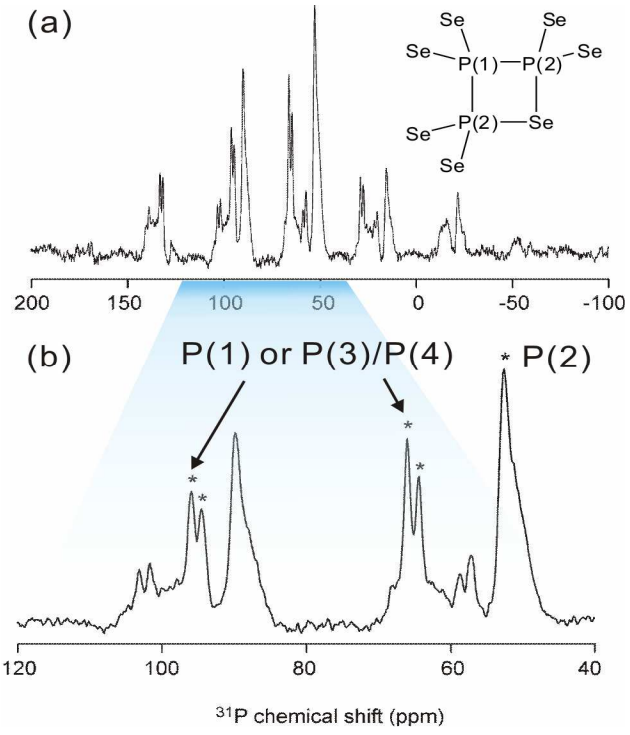

References

(1) Chung, I.; Song, J.-H.; Jang. I. J.; Freeman, A. J.: Ketterson, J. K.; Kanatzidis, G. *J. Am. Chem. Soc*. **2009**, *131*, 2647-2656, and references therein.

(2) Chung, I.; Karst, A. L.; Weliky, D. P.; Kanatzidis, M. G. *Inorg. Chem*. **2006**, *45*, 2785.

(3) Chung, I.; Jang, J. I.; Gave, M. A.;Weliky, D. P.; Kanatzidis, M. G. *Chem. Commun*. **2007**, 4998.